Impact of the 2019/2020 Australian megafires on Air Quality and Health

Ailish M Graham[1], Kirsty J. Pringle[1], Richard J Pope[1], Steve Robert Arnold[1], Luke Conibear[2], Helen Burns[1], Richard Rigby[1], Nicolás Borchers-Arriagada[3], Edward William Butt[1], Laura Kiely[1], Carly Lauren Serena Reddington[2], Dominick Vincent Spracklen[1], Matthew Thomas Woodhouse[4], Christoph Knote[5], and James B McQuaid[1]

[1]University of Leeds
[2]Institute for Climate and Atmospheric Science, School of Earth and Environment, University of Leeds
[3]Menzies Institute for Medical Research
[4]Commonwealth Scientific and Industrial Research Organisation (CSIRO)
[5]University of Augsburg, Germany

November 24, 2022

Abstract

The Australian 2019/2020 bushfires were unprecedented in both their extent and intensity, causing a catastrophic loss of habitat and human and animal life across eastern-Australia. Between October 2019 and February 2020 hundreds of fires burned, peaking in size in December and January and releasing the equivalent of half of Australia's annual carbon dioxide (CO2) emissions. We use a high-resolution atmospheric-chemistry transport model to assess the impact of the bushfires on particulate matter with a diameter less than 2.5 µm (PM2.5) concentrations across eastern Australia. The health burden from short-term population exposure to PM2.5 is then quantified using a concentration response function. We find that between October and February an additional ˜1.9 million people in eastern-Australia were exposed to 'Poor', 'Very Poor' and 'Hazardous' air quality index levels due to the fires. The impact of the bushfires on AQ was concentrated in the cities of Sydney, Newcastle-Maitland and Canberra-Queanbeyan during November, December and, also in Melbourne, in January. The health burden of bushfire PM2.5 across eastern-Australia, regionally and at city level is also estimated. Our estimate indicates that between October and February 171 (95% CI: 66 – 291) deaths were brought forward. The health burden was largest in New South Wales (109 (95% CI: 41 – 176) deaths brought forward), Queensland (15 (95% CI: 5 – 24)) and Victoria (35 (95% CI: 13 – 56)). At a city level the health burden was concentrated in Sydney (65 (95% CI: 24 – 105)), Melbourne (23 (95% CI: 9 – 38)) and Canberra-Queanbeyan (9 (95% CI: 4 – 14)), where large populations were exposed to high PM2.5 concentrations due to the bushfires.

Impact of the 2019/2020 Australian megafires on Air Quality and Health

Ailish M. Graham[1], Kirsty J. Pringle[1], Richard J. Pope[1,2], Stephen R. Arnold[1], Luke A. Conibear[1], Helen Burns[1,3], Richard Rigby[1,3], Nicolás Borchers-Arriagada[4], Edward W. Butt[1], Laura Kiely[1], Carly Reddington[1], Dominick V. Spracklen[1], Matthew T. Woodhouse[5], Christoph Knote[6], James B. McQuaid[1]

[1] School of Earth and Environment, University of Leeds, Leeds, LS2 9JT, UK

[2] National Centre for Earth Observation, University of Leeds, Leeds, LS2 9JT, UK

[3] Centre for Environmental Modelling and Computation, University of Leeds, Leeds, LS2 9JT, UK

[4] Menzies Institute for Medical Research, University of Tasmania, Hobart, TAS 7000 Australia

[5] Commonwealth Scientific and Industrial Research Organisation, Aspendale, Victoria, Australia

[6] Model-Based Environmental Exposure Science, Faculty of Medicine, University of Augsburg, Germany

Correspondence to: Ailish M. Graham (ee15amg@leeds.ac.uk)

Key Points:

- ~1.9 million people were exposed to 'Poor', 'Very Poor' or 'Hazardous' air quality index levels in eastern-Australia due to the fires.
- The bushfire PM2.5 health burden was largest in NSW (109 (95% CI:41-176)), Queensland (15 (95% CI:5-24)) and Victoria (35 (95% CI:13-56)).
- The health burden was concentrated in Sydney (65 (95% CI:24-105)), Melbourne (23 (95% CI:9-38)) and Canberra-Queanbeyan (9 (95% CI:4-14)).

Abstract

The Australian 2019/2020 bushfires were unprecedented in both their extent and intensity, causing a catastrophic loss of habitat and human and animal life across eastern-Australia. Between October 2019 and February 2020 hundreds of fires burned, peaking in size in December and January and releasing the equivalent of half of Australia's annual carbon dioxide (CO_2) emissions. We use a high-resolution atmospheric-chemistry transport model to assess the impact of the bushfires on particulate matter with a diameter less than 2.5 μm ($PM_{2.5}$) concentrations across eastern Australia. The health burden from short-term population exposure to $PM_{2.5}$ is then quantified using a concentration response function. We find that between October and February an additional ~1.9 million people in eastern-Australia were exposed to 'Poor', 'Very Poor' and 'Hazardous' air quality index levels due to the fires. The impact of the bushfires on AQ was concentrated in the cities of Sydney, Newcastle-Maitland and Canberra-Queanbeyan during November, December and, also in Melbourne, in January. The health burden of bushfire $PM_{2.5}$ across eastern-Australia, regionally and at city level is also estimated. Our estimate indicates that between October and February 171 (95% CI: 66 – 291) deaths were brought forward. The health burden was largest in New South Wales (109 (95% CI: 41 – 176) deaths brought forward), Queensland (15 (95% CI: 5 – 24)) and Victoria (35 (95% CI: 13 – 56)). At a city level the health burden was concentrated in Sydney (65 (95% CI: 24 – 105)), Melbourne (23 (95% CI: 9 – 38)) and Canberra-Queanbeyan (9 (95% CI: 4 – 14)), where large populations were exposed to high $PM_{2.5}$ concentrations due to the bushfires.

1 Introduction

The Australian 2019/2020 bushfires were unprecedented in both their extent and intensity (Brew et al., 2020), causing a catastrophic loss of habitat and human and animal life. Between October 2019 and February 2020 hundreds of fires burned in the south-east of the country, peaking in size in December and January. By burned area the bushfires were the largest in south-east Australia since European occupation (late 1700s) (Wintle et al., 2020), burning more than 10 million hectares of vegetation. The burned area of the 2019/2020 fires was larger than the Ash Wednesday (1983) and Black Saturday (2009) fires combined (Brew et al., 2020). The immediate impacts of the bushfires included the destruction of almost 6,000 buildings and the deaths of 34 people and more than three billion terrestrial vertebrates (Verzoni, 2021).

The severity of the 2019/2020 bushfire season was promoted by a decrease in rainfall and increase in temperatures due to a combination of meteorological and climatic conditions (Australian Bureau of Meteorology, 2019a). Australia had experienced two consecutive very dry years prior to 2019 (2017-2018), with 2019 being the warmest and driest on record (van Oldenborgh et al., 2020). This was combined with a strong positive Indian Ocean Dipole (IOD) phase from July 2019 onwards (Australian Bureau of Meteorology, 2020) and a negative Southern Annular Mode (SAM) event (Australian Bureau of Meteorology, 2019b), both of which reduce rainfall across south-eastern Australia.

The vegetation cover in east Australia is dominated by native tree and grass species (native forests and woodlands, native shrublands and heathlands, native grasslands and minimally modified pasture), annual crops and highly modified pastures (Australia State of the Environment, 2016). The forests are temperate broadleaf and are principally eucalypts, one of the most fire prone species in the world. Fires in eucalypt forests spread largely through the leaf litter layer, and the dryness of this layer effectively controls the occurrence of fires (Boer et al., 2020). In 2019, the moisture content of leaf litter reached record low levels and the total area of leaf litter exceeded critical flammability levels; being the highest in the past 30 years (van Oldenborgh et al., 2020). Typically, <2% of eucalypt forests burn in the most extreme fire seasons (Boer et al., 2020). However, during the 2019/2020 bushfires 21% of the biome burned, well above the burned percentages seen anywhere else in the world.

Emissions from the bushfires also had a large impact at a global scale, releasing >300 tonnes of CO_2 between August and January, equivalent to half of Australia's annual carbon emissions (Lee, 2019). In addition, the fires produced large-scale enhancements in trace gases over a large region of the South Pacific, and plumes from the fires (carbon monoxide) circumnavigated the Southern hemisphere (Jenner, 2020; Pope et al., 2021).

Substantial epidemiological and toxicological evidence supports the association between wildfire $PM_{2.5}$ exposure and short-term all-cause mortality and short-term respiratory morbidity (Delfino et al., 2009; Faustini et al., 2015; Johnston et al., 2011; Naeher et al., 2007; Reid et al., 2016; Zanobetti and Schwartz, 2009). However, research to identify the toxicity of different components of $PM_{2.5}$ chemical composition is ongoing, and so equal toxicity for all $PM_{2.5}$ is commonly assumed in health impact assessments. The health burden of wildfires is concentrated in the tropics, Australia, Canada and the USA and is substantial (Black et al., 2017; Crippa et al., 2016; Johnston et al., 2012; Liu et al., 2015; Reid et al., 2016). The $PM_{2.5}$ associated health burden from long-term exposure is dominated by exposure to wildfires in large parts of these countries (Lelieveld et al., 2015). Therefore, reducing population exposure to pollutants from wildfires is likely to yield an near-term, large health benefit in these regions (Johnston et al., 2012).

Climate change is projected to increase the frequency, intensity and spread of wildfires both globally (Sutton et al., 2011) and in Australia (Lucas et al., 2007). Fire weather conditions in Australia are predicted to worsen, with forest fire danger index (FFDI) projected to increase in all climate change scenarios (0-10% by 2020 and 0-30% by 2050) (Lucas et al., 2007). Alongside this, the number of days where fire danger is 'very-high' or 'extreme' was projected to increase by between 5-65% by the end of 2020, with an increase in the length of the fire season (Lucas et al., 2007). The largest changes in FFDI were predicted to be seen in New

South Wales due to the Mediterranean climate of the region. Mild, wet winters encourage the growth of fuel, and hot, dry summers lead to an increase in the FFDI (Lucas et al., 2007). The increase in bushfire frequency and intensity is likely to increase population exposure to pollutants from bushfires, and therefore the health burden of bushfire events.

The first study to investigate the impact of the 2019/2020 bushfires on mortality from exposure to $PM_{2.5}$ used $PM_{2.5}$ concentrations observed at ground-based air quality monitoring sites across eastern Australia to estimate daily mean $PM_{2.5}$ exposure (Borchers Arriagada et al., 2020). Inverse distance weighting was used to interpolate $PM_{2.5}$ monitoring data spatially to statistical area level 2 (SA2s) centroids within 100 km of each monitoring site. SA2s generally include a population of ~10,000 (3,000 – 25,000) and are designed to be representative of individual communities that interact together socio-economically. The entire SA2 population was then assumed to be exposed to the interpolated $PM_{2.5}$ concentration. Bushire smoke affected days were defined, for each monitoring site, as days where the daily mean $PM_{2.5}$ concentration exceeded the 95th percentile of historical daily mean $PM_{2.5}$ concentrations. The contribution of bushfire smoke to the total $PM_{2.5}$ mass (bushfire smoke $PM_{2.5}$) was estimated using the difference between the observed $PM_{2.5}$ concentration and the long-term historical monthly-mean $PM_{2.5}$ concentration at each monitoring site. Using the bushfire smoke $PM_{2.5}$ the health impacts of bushfire $PM_{2.5}$ exposure were estimated, applying the WHO (2013) short-term exposure-response function for all-cause, all-age mortality. The estimated health impact on mortality was substantial, with an estimated 417 (95% CI: 153 – 680) deaths brought forward across eastern-Australia due to bushfire smoke between October 1st 2019 and February 10th 2020. The health impact on mortality was highest in New South Wales and Victoria (219 (95% CI: 81 – 357) and 120 (95% CI: 44 – 195)).

In a separate study, Ryan *et al.* (2021) used a random forest model, trained using ground-based observations, to predict air pollutant concentrations, including $PM_{2.5}$, without bushfires. These were compared with ground-based observations during the period of the bushfires to estimate the bushfire contribution to $PM_{2.5}$ concentrations each day. Population-weighted bushfire $PM_{2.5}$ exposure and short-term health impacts in New South Wales and Victoria were then estimated in the same way as Borchers Arriagada *et al.* (2020). The estimated health impact lay within the lower limit of Borchers Arriagada *et al.* (2020) in New South Wales and Victoria at 152 (95% CI: 95 – 209) and 92 (95% CI: 57 – 126), compared with 219 (95% CI: 81 – 357) and 120 (95% CI: 44 – 195). The difference was attributed to the different approaches to quantifying the bushfire fraction of $PM_{2.5}$, as well as the study by Ryan *et al.* (2021) only including populations within the large cities (~80% of the region) rather than the entire region population.

This paper will use an atmospheric chemistry transport model (ACTM) to explicitly simulate $PM_{2.5}$ concentrations between September 1st 2019 and January 31st 2020 at 30 km resolution. This aims to provide a more accurate daily estimation of the bushfire smoke contribution to total $PM_{2.5}$ mass, by simulating $PM_{2.5}$ concentrations accounting for real time meteorological conditions and atmospheric processes, and calculating explicitly the $PM_{2.5}$ increment due to the fires. Regional population exposure is likely to be better captured, since this is more challenging to capture using sparse monitoring network that may not capture strong $PM_{2.5}$ concentration gradients which are likely to have been observed during the fire event. This allows us to estimate the health impacts of bushfire $PM_{2.5}$ exposure at both city and region-wide scales.

2 Materials and Methods

2.1 Model Description

$PM_{2.5}$ concentrations between September 1st 2019 to January 31st 2020 were simulated using the Weather Research and Forecasting model coupled to Chemistry (WRF-Chem) model (version 3.7.1), a fully coupled atmospheric chemistry model. A detailed model description can be found in Conibear *et al*. (2018a), and this model version has been used to successfully simulate $PM_{2.5}$ air pollution for India (Conibear et al., 2018a, 2018b, 2018c), SE Asia (Kiely et al., 2020, 2019), and China (Reddington et al., 2019; Silver et al., 2020). The model domain covered eastern-Australia (128.9 to 170.6°E and -9 to -48°N) at 30 km horizontal resolution (130x150 grid boxes), with 33 vertical levels (up to 10 hPa) and included 89% (22.1 m) of the Australian population. The contribution of bushfires to surface $PM_{2.5}$ concentrations between September 1st and January 31st was calculated by simulating two scenarios, with and without fire emissions. This allowed the contribution of the fires to air quality and health be quantified ($PM_{2.5\ Fires}$ - $PM_{2.5\ No\ Fires}$ = $PM_{2.5\ Fires\ Only}$).

Meteorological conditions were initialised using ERA5 6-hourly analyses at 0.1° resolution on 38 pressure levels (Hoffmann et al., 2018). Nudging was used in order to keep simulated meteorology in line with the meteorological analyses. Several nudging sensitivity experiments were carried out to investigate the sensitivity of simulated $PM_{2.5}$ concentrations to the nudging option used **(**Supplementary Material: Figure S4). Nudging of potential temperature, the horizontal and vertical winds and the water vapour mixing ratio in all vertical levels, rather than just above the boundary layer, improved simulated $PM_{2.5}$ concentrations by reducing the Root Mean Square Error (RMSE) to 22.9 $\mu g\ m^{-3}$ from 24.1 $\mu g\ m^{-3}$, Normalised Mean Absolute Error (NMAE) to 0.72 from 0.74 and Normalised Mean Bias (NMB) to -0.17 from -0.49, respectively. Though the Pearson correlation coefficient (r) was slightly reduced to 0.39 from

0.42 (Supplementary Material: Table S1). Therefore, the results of the simulations where all meteorological variables in all vertical levels were nudged are presented here.

Chemical boundary conditions were provided by the Whole Atmosphere Community Climate Model (WACCM) 6-hourly simulation data (Marsh et al., 2013; UCAR, 2020a). WACCM meteorology is driven by the NASA Global Modelling and Assimilation Office (GMAO) Goddard Earth Observing System Model (GEOS-5) model. Anthropogenic emissions for 2014 from the Community Emissions Data System (CEDS) (used in the 6^{th} Coupled Model Intercomparison Project (CMIP6)) and the Fire Inventory from NCAR (FINN) version 1 (v1) fire emissions are used in WACCM. Model output is given on 88 vertical levels at 0.9x1.25º (UCAR, 2020b).

Global anthropogenic emissions were taken from the Emission Database for Global Atmospheric Research with Task Force on Hemispheric Transport of Air Pollution version 2.2 (EDGAR-HTAP2) (Janssens-Maenhout et al., 2015) at 0.1° resolution for 2010. Sector specific diurnal cycles were subsequently added to the emissions, using diurnal cycles from Olivier *et al.* (2003). EDGAR-HTAP2 is a global, gridded, air pollution emission inventory compiled of officially reported, national gridded inventories. Where national emissions datasets or specific sectors are not available 2010 EDGAR v4.3 grid maps are used. Emissions include SO_2, NO_x, CO, NMVOC, NH_3, PM_{10}, $PM_{2.5}$, BC and OC. Emissions include all anthropogenic emissions except large-scale biomass burning (e.g. wildfires).

The Model for Ozone and Related Chemical Tracers, version 4 (MOZART-4) (Emmons et al., 2009) is used to calculate gas-phase chemical reactions. Aerosol chemistry and physics are represented using the Model for Simulating Aerosol Interactions and Chemistry (MOSAIC) scheme, with sub-grid scale aqueous chemistry (Zaveri et al., 2008). Aerosols are represented by four sectional discrete size bins (0.039–0.156 μm, 0.156–0.625 μm, 0.625–2.5 μm, 2.5–10 μm). The use of the MOSAIC scheme balances detailed chemistry with computational expense.

2.1.1 Wildfire emissions

Wildfire emissions are taken from FINNv1 near-real time (FINNv1 NRT), since FINNv1.5 was not available at the time model simulations were carried out. FINN combines satellite observations, land cover, biomass consumption estimates and emissions factors to calculate daily fire emissions globally at 1 km resolution. FINN uses satellite observations from the MODIS Thermal Anomalies Product to provide detections of active fires. Burned area is assumed to be 1 km^2 for each fire identified and scaled back based on the density of vegetation from the MODIS Continuous Fields (VCF) (i.e. if 50% bare = 0.5 km^2 burned area). The type of vegetation burned during a detected fire is determined using the MODIS Collection 5 Land Cover Type (LCT). This assigns each fire pixel to one of 16 possible land cover/land use classes and also the density of vegetation at 500 m resolution, scaled to 1 km. The 16 land cover types are then aggregated into 8 generic categories to which fuel loadings are applied (Wiedinmyer et al., 2011). Fuel loadings are from Hoelzemann *et al.* (2004) and emissions factors are from Akagi *et al.* (2011), Mcmeeking (2008) and Andrae and Merlet (2001). Fire types included are wildfires, prescribed and agricultural burning. However, trash burning or biofuel use are not included.

The key difference between FINN v1 NRT and FINN v1.5 is that FINN v1 NRT uses MODIS near real time fire counts rather than the reprocessed fire counts, which FINN v1.5 uses. The differences between the two datasets over Australia for the year 2018 (and 2019 following the v1.5 release) are quantified (Supplementary Material: Figure S1) to identify any differences in emissions. Generally, emissions for 2019 indicate that emissions per fire hotspot were much higher than previous years (2010-2018). This is likely due to the high levels of dry fuel availability during 2019 (van Oldenborgh et al., 2020). Emissions in FINN v1.5 and NRT are in good agreement for 2018, while for 2019 FINN NRT $PM_{2.5}$ (~1 Tg) are slightly higher than FINNv1.5 (~0.9 Tg). However, there is a much larger range of disagreement in the estimates of 2019 annual fire emissions between the five key fire emissions datasets (~1 to >7.5 Tg) (Supplementary Material: Figure S2). Due to the large discrepencies in annual fire emission estimates from the five key fire emission datasets available, we also carry out a further simulation where FINN NRT emissions are scaled by 1.5 (referred to later as scaled_1.5) to test the sensitivity of simulated $PM_{2.5}$ concentrations to total fire emissions.

Release of Fire Emissions

The high temperatures associated with combustion mean that wildfires can often inject emissions above the surface due to buoyancy of the fire plume. In WRF-Chem a default plume-rise parameterization is used to release fire emissions (Freitas et al., 2007). However, several studies have found that the plume-rise parameterization potentially represents an incorrect vertical distribution of the emissions (Archer-Nicholls et al., 2015; Crippa et al., 2016). Kiely *et al.* (2020, 2019) found that releasing emissions evenly through the boundary layer (BL) improved agreement between simulated surface $PM_{2.5}$ concentration and observations for Indonesian fires. Therefore, we test two options: 1) releasing emissions evenly through the boundary layer and 2) plume-rise. The results of this sensitivity study indicate that simulated $PM_{2.5}$ concentrations are relatively insensitive to the emission option used (Supplementary Material: Figure S4**)** but releasing emissions evenly through the BL performs better. Therefore, we present the results of releasing emissions evenly through the BL in this study.

2.2 Observations

Ground-based monitoring sites

Daily mean $PM_{2.5}$ mass concentrations, calculated from hourly $PM_{2.5}$ observations, at ground-based monitoring sites are used to assess model performance in simulating $PM_{2.5}$ concentrations. Data from the New South Wales, Queensland, Australian Capital Territory Government and the Victoria EPA monitoring networks were combined, providing data across 80 observational sites. A map of sites used is available in the Supplementary Material (Supplementary Material**:** Figure S3). Daily means were calculated from hourly data if >18 hours of data was available each day, otherwise a missing data flag was applied. Model performance was evaluated using r, NMB, RMSE and NMAE (Supplementary Material: Table S1). Multiple observations were available in several large cities (Newcastle, Sydney, Canberra, Melbourne – see Figure 1 for locations), allowing the model performance to be evaluated in locations where populations are likely to have been exposed to high concentrations of $PM_{2.5}$.

2.2.1 Health Impact Assessment

The health impact from short-term exposure to elevated $PM_{2.5}$ from the Australian fires is calculated using a concentration-response function (CRF). The CRF of the World Health Organisation (2013) was used to estimate the impact of short-term exposure to $PM_{2.5}$ on mortality.

$$E_m = \sum_{i=1}^{N} B_d . pop_i . AF_i \tag{1}$$

Here, E_m represents the excess mortality caused by exposure to $PM_{2.5}$ over the theoretical minimum risk level of exposure (Equation ((*3*): $\Delta X – X_0$) each day. N is the number of days within the simulation and i is the day in simulation, B_d is the baseline death rate, pop_i is the population exposed each day and AF_i is the attributable fraction of risk each day due to exposure to $PM_{2.5}$.

$$AF = \left(\frac{RR - 1}{RR}\right) \quad (2)$$

$$RR = \exp^{\beta(\Delta X - X_0)} \quad (3)$$

The AF is calculated using the concept of relative risk (RR), which is the probability of mortality from a disease endpoint within an exposed population compared to within an unexposed population. The concentration of bushfire $PM_{2.5}$ a population is exposed to is given by ΔX ($PM_{2.5\ FIRES}$ - $PM_{2.5\ NO\ FIRES}$) and the safe- limit of exposure is X_0. Since there is little evidence to suggest a safe-limit of exposure to $PM_{2.5}$ we assume X_0 to be zero (Holgate, 1998; Macintyre et al., 2016; Schmidt et al., 2011).

$$\beta = \frac{\ln(RR)}{\Delta C} \quad (4)$$

We use relative risk values from the World Health Organisation (2013) of 1.0123 (95% CI: 1.0045, 1.0201) per 10 μg m^{-3}, which we use to estimate beta (ß) using Equation (4). Since the RR used is for all-cause, all-age mortality, we use all-cause, all-age baseline mortality rates in the calculations. Calculated health impacts are separated by region and city using shapefiles.

2.2.1 Population and Baseline Mortality Data

Population count data for 2018 is from the Australia Bureau of Statistics (Australian Bureau of Statistics, 2019) at 1 km resolution. This indicates our model domain includes 89% of the Australian population. Baseline all-cause, all-age 2018 mortality rate data for each region in our model domain is taken from the Australia Bureau of Statistics (Australian Bureau of Statistics, 2020) (Supplementary Material: Table S6).

3 Results

3.1 Fire Emissions

FINN emissions clearly indicate that the $PM_{2.5}$ emissions between late-October 2019 and mid-January 2020 were unprecedented, lying far above the daily mean emissions observed in the previous 8 years (Figure 1 and Supplementary Material: Table S1). The Australian bushfires in 2019-2020 began in the northern region of eastern-Australia (close to Brisbane and Newcastle) and shifted south through the season (Figure 1). As the fires moved southwards, $PM_{2.5}$ emissions also increased, with the highest $PM_{2.5}$ emissions occurring in south-eastern Australia in late December- early January.

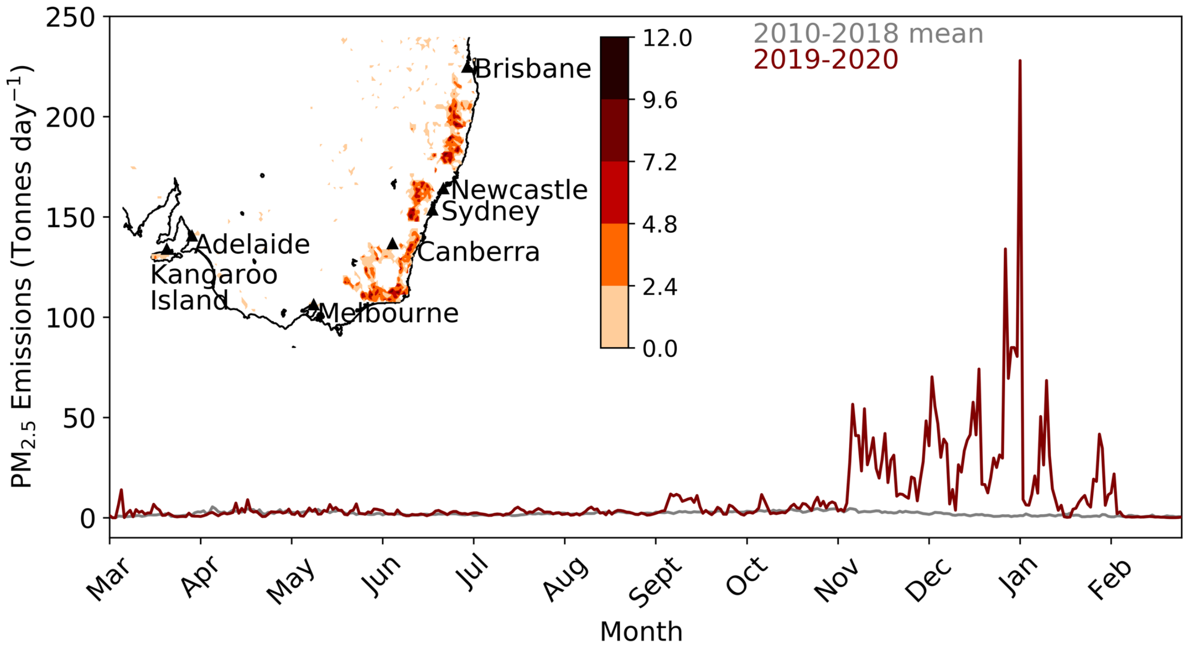

Figure 1. $PM_{2.5}$ fire emissions (Tonnes day^{-1}) across Australia between March 2019 and March 2020 from the FINN near-real time fire emission dataset. The timeseries shows the 2010-2018 daily mean $PM_{2.5}$ emissions (grey) and the 2019-2020 daily mean $PM_{2.5}$ emissions (maroon). Inset map: Map of total $PM_{2.5}$ fire emissions (Tonnes km^{-2}) across eastern Australia between March 2019 and March 2020.

The impact of the fires on $PM_{2.5}$ air quality (AQ) is clear from ground-based observations across south-east Australia (Figure 2). Observations indicate that between October 2019 and February 2020 daily mean $PM_{2.5}$ concentrations averaged across all sites reached 70 μg m^{-3} on several days. In the no fires simulation concentrations remain below 20 μg m^{-3}, indicating that a large fraction of the total $PM_{2.5}$ mass observed is due to fires. The impact of the fires on populations can be more clearly seen when $PM_{2.5}$ concentrations in individual cities are examined (Figure 2). Newcastle and Sydney exhibit the same pattern of $PM_{2.5}$ variability, following the pattern seen regionally across eastern-Australia closely. High $PM_{2.5}$ concentrations are first observed in late October and affect the cities sporadically until mid-January, reaching ~75 μg m^{-3}. In contrast, the impacts of the fires on $PM_{2.5}$ AQ in Canberra are not seen until November and December. However, concentrations are much higher in Canberra, reaching >100 μg m^{-3} in November and >300 μg m^{-3} in December. $PM_{2.5}$ AQ in Melbourne is affected latest, with $PM_{2.5}$ concentrations reaching 50 to >150 μg m^{-3} in December and January.

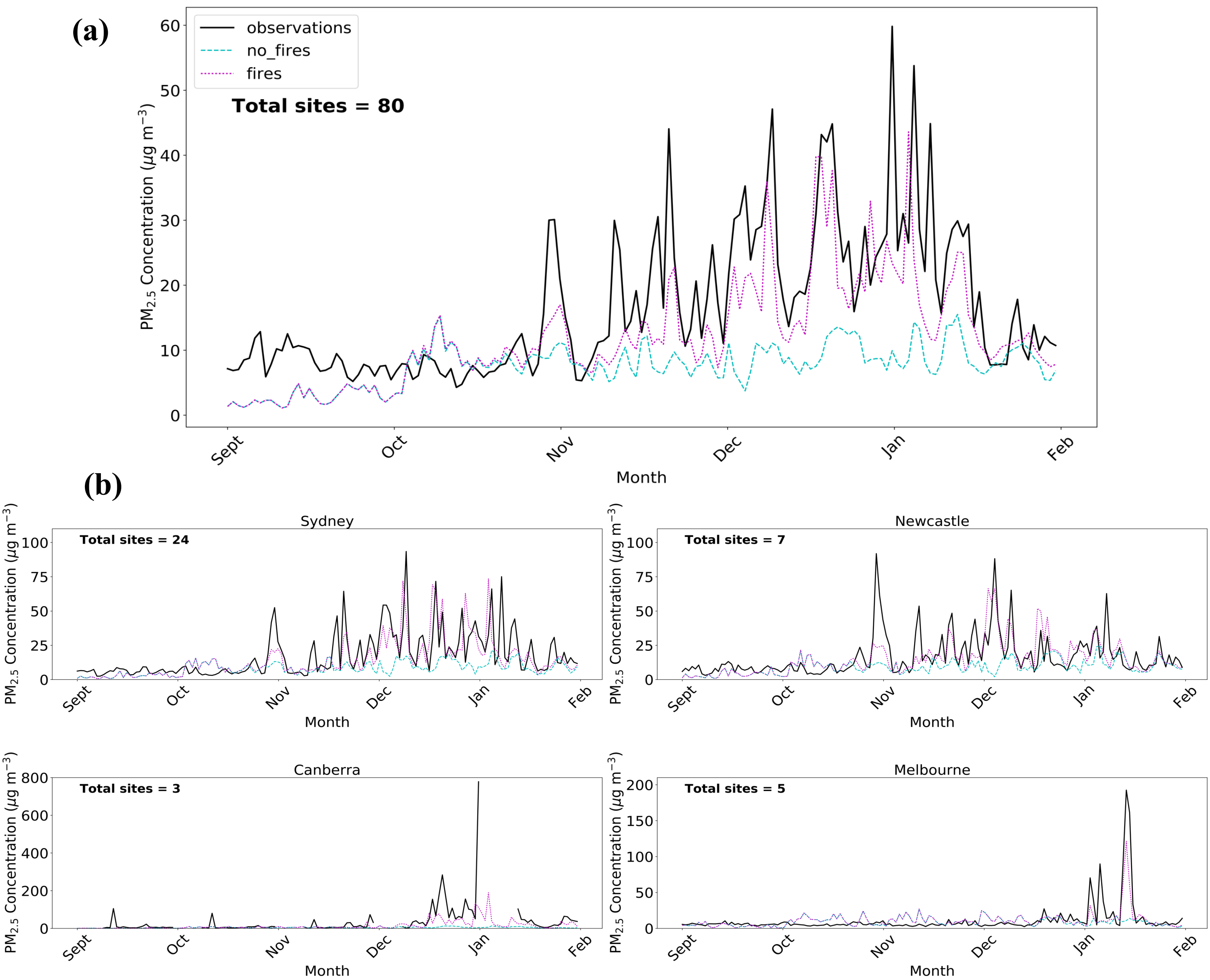

Figure 2. (a) Observed (black) and simulated (dotted magenta and dashed cyan) daily mean $PM_{2.5}$ concentrations. Simulations shown are no fires (dashed cyan) and fires (dotted magenta). The mean $PM_{2.5}$ concentration from all 80 observational sites across eastern-Australia is shown for the model and observations. (b) The same as above but for individual cities (Sydney, Newcastle, Canberra and Melbourne). The observed (black) and simulated (dotted magenta and dashed cyan) daily mean $PM_{2.5}$ concentrations are shown for each city. The total number of observational sites in each city is also shown on the left of each panel.

3.2 Model Evaluation

Evaluation of the WRF-Chem model indicates that the model generally underestimates $PM_{2.5}$ in early September (by ~70%) but then tends to overestimate $PM_{2.5}$ (by ~30%) in early October (before the fires) across all sites (Figure 2). This is also generally true at city scale (Figure 2). During the fire period (late-October – November) there is a substantial enhancement in $PM_{2.5}$ in both the observations and WRF-Chem fires simulation. The fires simulation captures the variability in $PM_{2.5}$ observations reasonably well (r=0.39), particularly compared to the no fires simulation (r=0.14). The fires simulation also captures the concentrations observed in the peaks and ambient conditions well (RMSE = 22.9 μg m^{-3}, NMB = -0.17), compared to the no fires simulation (RMSE = 25.3 μg m^{-3}, NMB = -0.45) and the scaled fire emissions simulation [scaled_1.5] (RMSE = 24.3 μg m^{-3}, NMB = -0.03), in which fire emissions between September and February were scaled by 1.5 (see Supplementary Material: Fire Emissions and Figure S2 for more details) . The model performs well in all of the cities, which have several observational sites (Sydney, Newcastle and Melbourne), capturing the variability and magnitude of the peaks in $PM_{2.5}$ well. The model struggles to capture the magnitude of the $PM_{2.5}$ peaks observed in Canberra but this is likely due to the lack of observations (3 sites), meaning the model struggles to represent a small number of point measurements. $PM_{2.5}$ concentrations in cities for which there are many more observation locations (5 - 24 sites) are represented better by the model. The improvement in model performance in cities where there are multiple observations gives confidence in the ability of the model to represent the population exposure to $PM_{2.5}$ from the fires.

Monthly mean modelled $PM_{2.5}$ concentrations from the fires and no fire runs can be used to understand the impact of the bushfires on $PM_{2.5}$ concentrations across south-east Australia (Figure S6, Figure S7 and Figure S8). This indicates that although monthly mean concentrations were relatively low in October and November (monthly mean ≤ 25 μg m^{-3}), a large fraction of $PM_{2.5}$ around Brisbane (20-30%) and also Newcastle and Sydney (20-100%) was from fires. This bushfire fraction increases in magnitude and spatial extent as the fires peak in December and January, when >70% of $PM_{2.5}$ is from fires over a large region including Melbourne, Canberra, Sydney, Newcastle and Brisbane.

3.3 Air Quality Impacts

Combining simulated $PM_{2.5}$ concentrations with population data (at 1 km) allows the contribution of the fires to population exposure to poor AQ to be estimated across eastern-Australia (Figure 3 (a)**,** Supplementary Material: Figure S9) and in individual cities (Figure 4 (a)). Across eastern-Australia exposure to New South Wales Air Quality Index (AQI) values before the fires (in September and October) were dominated by 'V.Good' and 'Good' values (Figure 3 (a) and Supplementary Material: Table S2). During September, on average, ~21.4 million people were exposed to 'V. Good' and 'Good' AQI concentrations **(**Supplementary Material: Table S2), while ~6,000 people were exposed to concentrations poorer than 'Good' AQI. In October, there was an increase in the monthly mean population exposure to poor $PM_{2.5}$ AQ ('Poor', 'V.Poor' and 'Hazardous' $PM_{2.5}$ AQI values) (Figure 3 (a)), however overall monthly mean exposure to poor AQ remained low. An average of 298,000, 12,100 and 93 people were exposed to 'Poor', 'V.Poor' and 'Hazardous' $PM_{2.5}$ AQI values. Throughout November exposure to poor AQ increased, exposing 1.35 m people to 'Poor' or 'V.Poor' $PM_{2.5}$ AQI (Figure 3). Between November 1st and February 1st the average population exposed to 'Poor', 'V.Poor' and 'Hazardous' $PM_{2.5}$ AQI values was ~1.5 m in November, 935,000 in December and ~1.3 m in January. This equates to a population ~2 times the size of Canberra-

Queanbeyan (~0.6 m) or almost half of the population of Brisbane (~3.5 m) being exposed to 'Poor' or worse AQ on average from November-February.

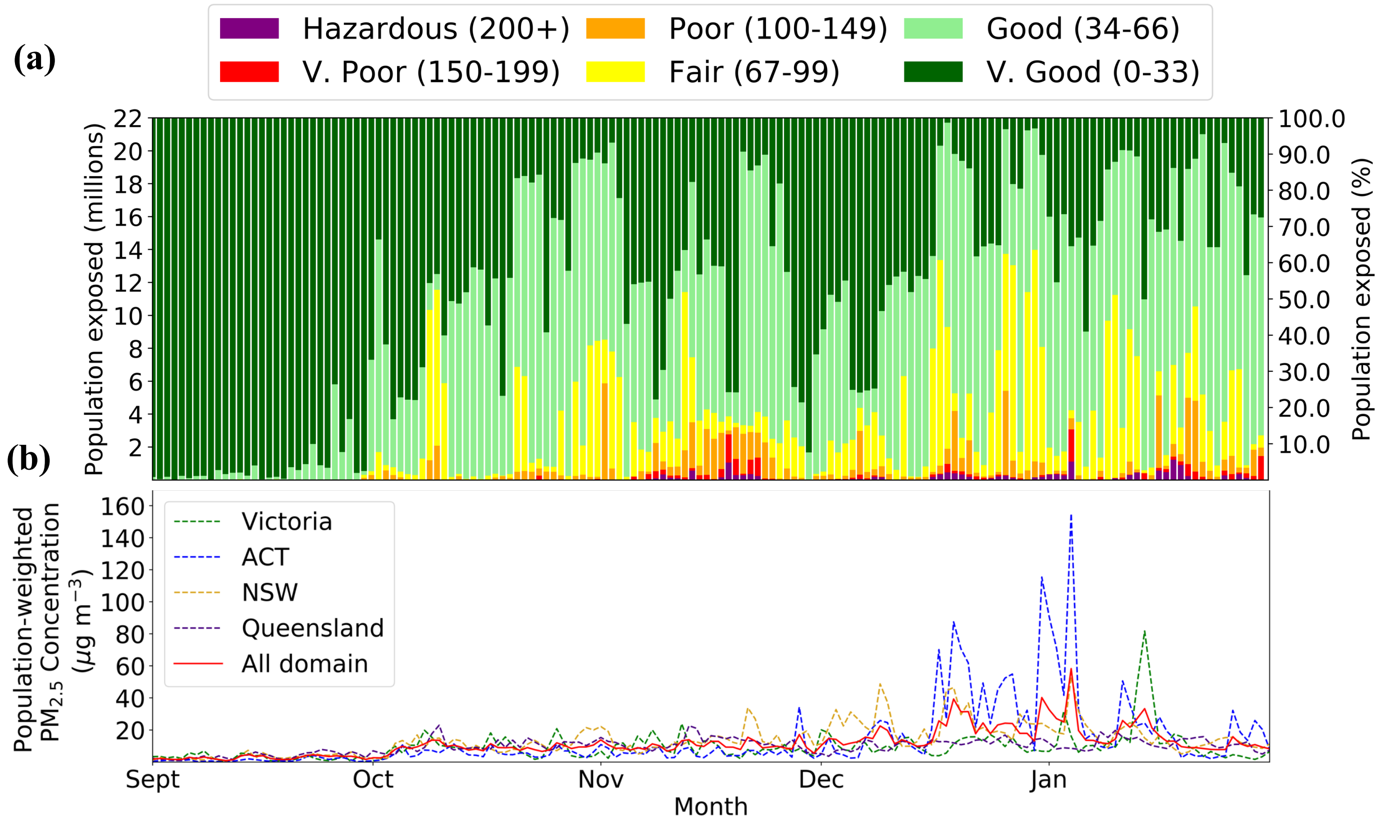

Figure 3. (a) Daily population exposure (in millions and %) to New South Wales Air Quality Index (AQI) values across eastern-Australia (fires simulation) between September 1st and January 31st. AQI values correspond to $PM_{2.5}$ concentrations of 0-8.5 (V. Good), >8.5-16.75 (Good), >16.75-25 (Fair), >25-37.5 (Poor), >37.5-50 (V. Poor), >50 (Hazardous), all in $\mu g\ m^{-3}$. More information on how the AQI is calculated is available in Supplementary Material: Table S9. (b) Daily population-weighted bushfire $PM_{2.5}$ exposure (in $\mu g\ m^{-3}$) across all states in the model domain (red) and regionally for Victoria (green), Australian Capital Territory blue (yellow) and Queensland (purple) (fires-no fires simulation) between September 1st and January 31st.

By comparing monthly mean population AQI exposure (calculated as the monthly mean AQI from the daily AQI) during the bushfires to if there were no fires (Supplementary Material: Table S2 and Table S3) exposure to high AQI value can be attributed to the fires rather than as a result of other effects (e.g. long-range transport of $PM_{2.5}$). This indicates that in the no fires simulation between September and the end of January in total 1.6 million people would have been exposed to 'Poor' AQI values, ~163,000 to 'V. Poor' AQI values and 130,000 to

'Hazardous' AQI values if there were no fires. Therefore, the fires led to an additional ~1.9 million people being exposed to 'Poor' or worse AQI values on average (~1.1 million exposed to 'Poor', 437,000 to 'V.Poor' and 339,000 to 'Hazardous' AQI values) across eastern Australia between September and February (Supplementary Material: Table S2 and Table S3).

In order to understand the impact of poor AQ from the fires on the population, the bushfire $PM_{2.5}$ concentration can be weighted by the total population in each region (population weighted bushfire $PM_{2.5}$). We calculate the population-weighted bushfire $PM_{2.5}$ concentration for the regions most severely affected by the fires (Figure 3 (b), Table 1 and Supplementary Material: Table S5). This indicates that the population in ACT was exposed to the highest $PM_{2.5}$ due to the fires. Here, population-weighted bushfire $PM_{2.5}$ concentrations reached 155.1 μg m^{-3} on January 4th and exceeded 100 μg m^{-3} on several days. This is far above the maximum population-weighted $PM_{2.5}$ concentrations in any of the other regions (Queensland (22.9 μg m^{-3}) NSW (53.4 μg m^{-3}) Victoria (81.8 μg m^{-3})) and far above the maximum between September 1st and January 31st across all regions, of 58.3 μg m^{-3}. The mean population-weighted $PM_{2.5}$ concentration between September and February across all regions was 11.6 μg m^{-3}, with the highest mean population-weighted $PM_{2.5}$ concentrations in ACT (14.1 μg m^{-3}) and NSW (13.4 μg m^{-3}). Comparing these results with Borchers Arriagada *et al.* (2020), population-weighted bushfire $PM_{2.5}$ concentrations are considerably lower in this study (Table 1 and Supplementary Material: Table S5). This is evident from the difference in the mean and maximum population-weighted $PM_{2.5}$ concentrations across all regions (mean: 11.6 μg m^{-3} vs 23.7 μg m^{-3} and maximum: 58.3 μg m^{-3} vs 98.5 μg m^{-3}). The disparity is dominated by the large differences between estimates for ACT and Victoria (Table 1 and Supplementary Material: Table S5), where observations were relatively sparse.

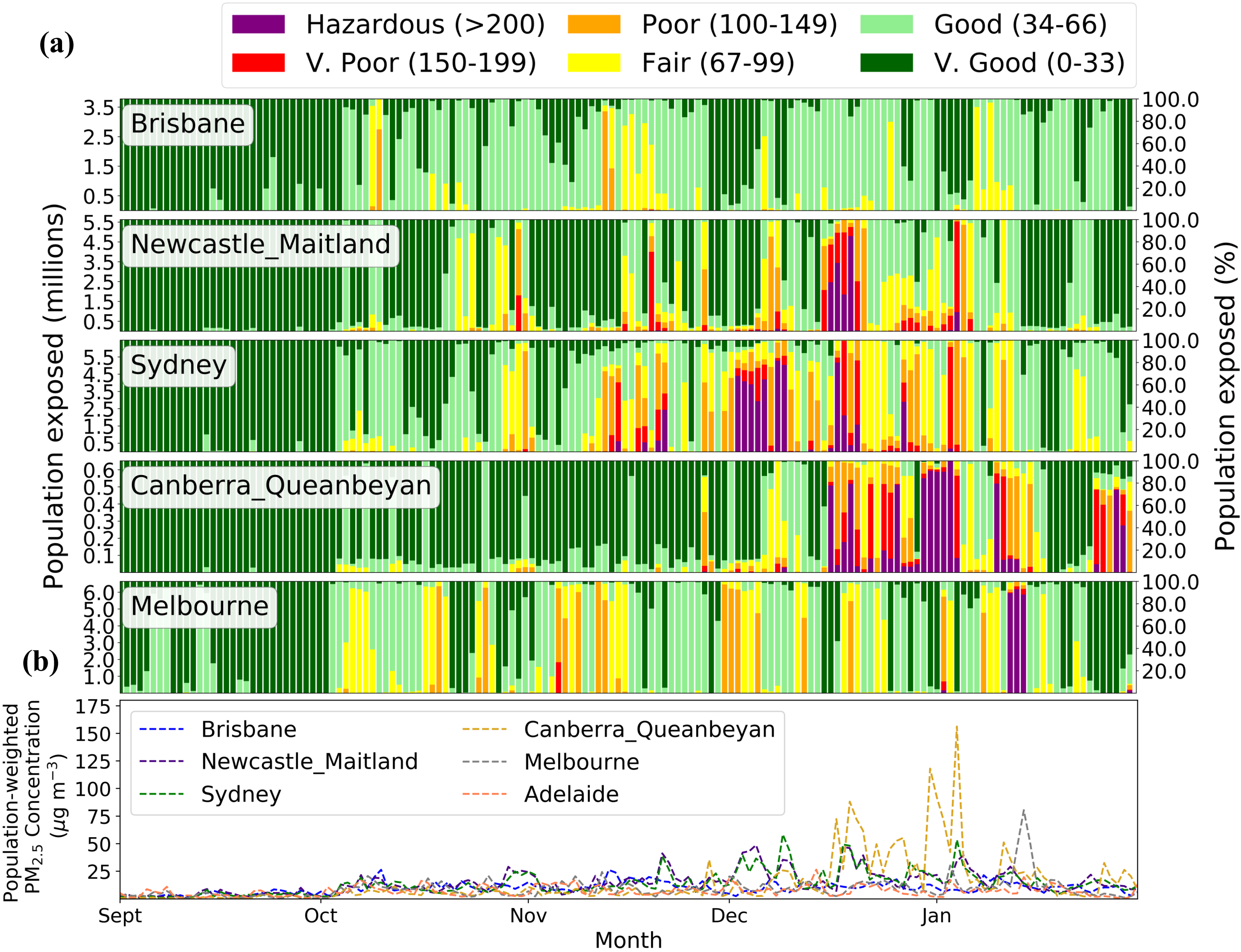

Figure 4. (a) Daily population exposure (in millions and % of total population) to New South Wales Air Quality Index (AQI) values in individual cities (Brisbane (Queensland), Sydney (NSW), Newcastle-Maitland (NSW), Canberra-Queanbeyan (ACT) and Melbourne (Victoria)) between September 1st and January 31st. AQI values correspond to $PM_{2.5}$ concentrations of 0-8.5 (V. Good), >8.5-16.75 (Good), >16.75-25 (Fair), >25-37.5 (Poor), >37.5-50 (V. Poor), >50 (Hazardous), all in µg m^{-3}.More information on how the AQI is calculatedis available in Supplementary Material: Table S9. (b) Daily population-weighted bushfire $PM_{2.5}$ concentration (in µg m^{-3}) in the cities of Brisbane (blue), Newcastle-Maitland (purple), Sydney (green), Canberra-Queanbeyan (yellow), Melbourne (grey) and Adelaide (orange) (fires- no fires simulation) between September 1st and January 31st.

When individual cities are considered (Figure 4 (a)) the effect of the southward shift of fires between October and January on population exposure to ‘Poor’, ‘V. Poor’ and ‘Hazardous’ $PM_{2.5}$ AQI can be clearly seen. In October, there is widespread exposure to ‘Poor’ $PM_{2.5}$ AQ. The effects of population exposure are largest in Brisbane, Newcastle-Maitland, Sydney and Melbourne with 93,000, 220,000, 49,000, and 468,000 people exposed to ‘Poor’ or worse $PM_{2.5}$ AQI values on average (Figure 4 (a) and Supplementary Material: Table S4). The impacts of fires on $PM_{2.5}$ AQ becomes most evident from November. During November average population exposure to ‘Poor’, ‘V. Poor’ and ‘Hazardous’ $PM_{2.5}$ AQ is evident in Sydney (112,000, 86,000 and 10,000 people exposed) and Newcastle-Maitland (235,000, 170,000, and 2,500 people exposed). Alongside this, in Canberra-Queanbeyan an average of 15,000, 1,100 and 174 people are exposed to ‘Poor’, ‘V. Poor’ and ‘Hazardous’ $PM_{2.5}$ AQI values in November. The pattern of increasing population exposure to poor $PM_{2.5}$ AQ continues in December, as the fires intensify, with a clear southward shift (Figure 4 (a)). Populations in Sydney, Newcastle-Maitland and Canberra-Queanbeyan continue to be exposed to ‘Poor’ and worse AQ. This leads to 3.6 m, 1.7 m and 237,000 people being exposed to ‘Poor’ or worse AQ in Sydney, Newcastle-Maitland and Canberra-Queanbeyan, respectively, on average in December (Supplementary Material: Table S4). During this time in Brisbane, Melbourne and Adelaide ~5,000, 1.1 m and 53,000 people on average are exposed to ‘Poor’ or worse AQ. Finally, in January, the southward shift in fires continues, with a clear decrease in exposure to ‘Poor’ or worse AQI in Brisbane, Sydney and Newcastle-Maitland but increases in monthly mean exposure to ‘Poor’ AQ in Canberra-Queanbeyan, Melbourne and Adelaide. This leads to 286,000, 979,000 and ~48,000 people being exposed to ‘Poor’, ‘V. Poor’ and ‘Hazardous’ $PM_{2.5}$ AQI values in Canberra-Queanbeyan, Melbourne and Adelaide on average (Supplementary Material: Table S4). Despite reductions in the total population exposed to hazardous AQI values in Newcastle-Maitland and Sydney, widespread population exposure to

'Poor', 'V. Poor' and 'Hazardous' $PM_{2.5}$ AQI values continues during January. On average 515,000 and ~820,000 people are exposed to 'Poor', 'V. Poor' and 'Hazardous' $PM_{2.5}$ AQI values in Newcastle-Maitland and Sydney in January (Supplementary Material: Table S4).

Population-weighted bushfire $PM_{2.5}$ (fires - no fires) for individual cities can be used to identify the cities most severely affected by bushfire-sourced $PM_{2.5}$ (Figure 4 (b), Table 1 and Supplementary Material: Table S5). In line with the region population-weighted $PM_{2.5}$ concentrations, Canberra-Queanbeyan (ACT) is affected most severely by $PM_{2.5}$ from the fires. Population-weighted $PM_{2.5}$ concentrations in Canberra-Queanbeyan reach 156.2 μg m^{-3} and average 14.2 μg m^{-3} between September 1st and January 31st. The maximum population-weighted $PM_{2.5}$ concentrations in Sydney (58.4 μg m^{-3}) and Newcastle-Maitland (48.7 μg m^{-3}) is much below Canberra-Queanbeyan. However, as a result of the prolonged exposure to poor AQ in Syndey and Newcastle-Matiland, the mean population-weighted $PM_{2.5}$ concentrations in both cities (13.8 μg m^{-3} and 14.3 μg m^{-3}) are similar to Canberra-Queanbeyan.

These results clearly indicate widespread population exposure to dangerous $PM_{2.5}$ AQI levels throughout November, December and January. This is likely to have a large impact on public health due to short-term exposure to high $PM_{2.5}$ concentrations. We estimate these effects in the next section.

Table 1. Mean and maximum (September 1st – January 31st) population-weighted $PM_{2.5}$ concentrations for regions and cities in eastern-Australia.

Region	**Mean Population-weighted $PM_{2.5}$ (μg m^{-3})**	**Maximum population-weighted $PM_{2.5}$ (μg m^{-3})**
Australian Capital Territory	14.1	155.1
New South Wales	13.4	53.4
Queensland	9.7	22.9
Victoria	9.1	81.8
All domain	11.6	58.3
City	**Mean Population-weighted $PM_{2.5}$ (μg m^{-3})**	**Maximum population-weighted $PM_{2.5}$ (μg m^{-3})**
Brisbane	9.7	26.4
Newcastle-Maitland	14.3	48.7
Sydney	13.8	58.4
Canberra-Queanbeyan	14.2	156.2
Melbourne	9.0	80.5
Adelaide	7.0	26.5

3.4 Health Impacts

Using the World Health Organisation (2013) concentration response function, the number of deaths brought forward due to $PM_{2.5}$ from the fires between October 1st and January 31st can be estimated using the concentration of $PM_{2.5}$ due to fires (i.e. the difference in $PM_{2.5}$ concentrations between the fires and no fires simulations) (Figure 5). This indicates the impact of short-term exposure to bushfire $PM_{2.5}$ has a substantial impact on health from mid-October to mid-January (Figure 5 (a)). In total 171 (95% CI: 64 – 277) deaths were brought forward as a result of $PM_{2.5}$ exposure from the bushfires (Supplementary Material: Health Impacts and Table S7) and 624 (95% CI: 230 – 1008) from exposure to all $PM_{2.5}$.

Regioanlly, the health impact of exposure to $PM_{2.5}$ was largest in New South Wales (NSW), Queensland and Victoria (Figure 5 (b)). We estimate that exposure to $PM_{2.5}$ between October and February led to 287 (95% CI: 107 – 463), 112 (95% CI: 41 – 181), and 155 (95% CI: 57 – 250) deaths being brought forward in New South Wales (NSW), Queensland and Victoria, respectively. Of these deaths, 109 (95% CI: 41-176), 15 (95% CI: 5-24) and 35 (95% CI: 13-56) deaths brought forward were due to exposure to $PM_{2.5}$ from the bushfires (Supplementary Material: Table S8). Comparing these estimates with the results of Borchers Arriagada *et al.* (2020) and Ryan *et al.* (2021) (Figure 5 (b)) the estimates in this study are within the range of both studies in NSW. We estimate 109 (95% CI: 41 – 176) deaths are brought forward by bushfire $PM_{2.5}$, while Borchers Arriagada *et al.* (2020) estimate 219 (95% CI: 81 – 357) and Ryan *et al.* (2021) estimate 152.1 (95% CI: 95 – 209). Our results lie below the lower end of estimates in Victoria at 35 (95% CI: 13 – 56) deaths brought forward by bushfire $PM_{2.5}$. This is considerably lower than Borchers Arriagada *et al.* (2020) estimate of 120 (95% CI: 44 – 195) and Ryan *et al.* (2021) estimate of 92 (95% CI: 57 – 126) deaths brought forward. All three studies use the same population, baseline mortality datasets and concentration-response function. Therefore, the disparity in results between the studies is likely due to a number of other factors. Firstly, our study uses modelled $PM_{2.5}$ concentrations, rather than observations. Since the model generally underestimates $PM_{2.5}$ concentrations, the overall health impact estimated is likely to be underestimated due to a reduction in population exposure to $PM_{2.5}$. Secondly, the bushfire fraction of the total $PM_{2.5}$ mass could be overestimated in the Borchers Arriagada *et al.* (2020) study due the use of monthly mean historical $PM_{2.5}$ concentrations to account for the no fire fraction of $PM_{2.5}$. This would lead to an overestimation in the health impact of bushfire $PM_{2.5}$. The estimate of Ryan *et al.* (2021), which used a random forest model to account for the non-bushfire $PM_{2.5}$ fraction, is also lower than Borchers Arriagada *et al.* (2020), further supporting this. Finally, this study uses modelled $PM_{2.5}$ concentrations to estimate $PM_{2.5}$ exposure rather than the inverse weighting method used to estimate $PM_{2.5}$ concentrations by Borchers Arriagada *et al.* (2020) and Ryan *et al.* (2021). The use of inverse weighting may struggle to account for meteorological or orographic effects on $PM_{2.5}$ concentration gradients. However, this is also a limitation in this study given the relatively coarse model resolution (30 km), which may also struggle to resolve the strong concentration gradients around cities and the fires.

When individual cities are considered in the health impact assessment it becomes clear that the health impact is concentrated in cities with high populations, where $PM_{2.5}$ concentrations due to fires were high (Figure 5 (c)). Of the large cities we investigated, the health impact of exposure to $PM_{2.5}$ from fires was largest in Sydney (65 (95% CI: 24 – 105)), Melbourne (23 (95% CI: 9 – 38)) and Canberra-Queanbeyan (9 (95% CI: 4 – 14)) (Figure 5, Supplementary Material: Table S8).

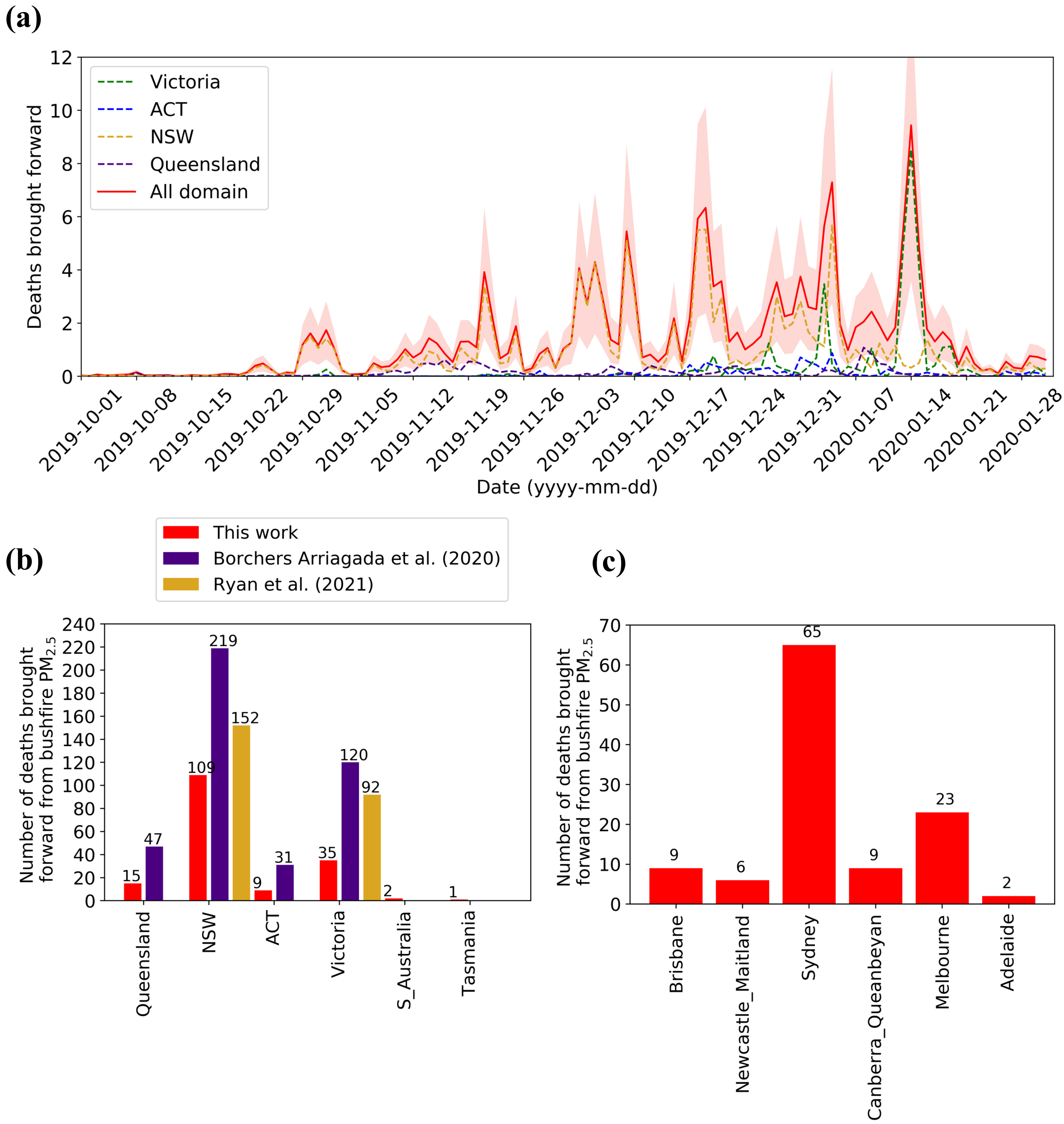

Figure 5. (a) Estimated increase in the number of deaths brought forward across model domain (red) and the regions of Victoria (green), Australia Capital Territory [ACT] (blue), New South Wales [NSW] (yellow) and Queensland (purple) due to $PM_{2.5}$ from bushfires (fires only) between October 1st and January 31st. Shading indicates the 95% confidence intervals of the estimate. The number of deaths brought forward due to bushfire $PM_{2.5}$ (fires only) (red) between October 1st and January 31st is also broken down by region (b) and city (c) and the total number of deaths is shown above the bars. The estimated number of deaths brought forward in each region (b) due to bushfire $PM_{2.5}$ (fires only) (red) in this study are compared to the Borchers Arriagada *et al.* (2020) (indigo) and Ryan *et al.* (2021) estimates for the same period.

4 Conclusions

We use the WRF-Chem regional air quality model to estimate the impact of the 2019/2020 Australian bushfires across eastern Australia, complementing the work of Borchers Arriagada *et al.* (2020) and Ryan *et al.* (2021), which were based solely on analysis of $PM_{2.5}$ observations. FINN fire emissions indicate $PM_{2.5}$ emissions from the 2019/2020 bushfires were unprecedented. Around 1 Tg of $PM_{2.5}$ was emitted from the fires during 2019 and ~0.3 Tg between January and February 2020. This is likely due to the high levels of dry fuel availability across the region during 2019 (van Oldenborgh et al., 2020).

Two model simulations were performed 1) with FINN fire emissions (fires) and 2) without FINN fire emissions (no fires), which allowed the impact of the bushfires on $PM_{2.5}$ air quality (AQ) and health to be quantified. Simulated $PM_{2.5}$ concentrations from the fires simulation reproduced observed daily mean concentrations relatively well but with a low bias (r = 0.39, RMSE = 22.9 μg m^{-3}, NMB = -0.17, NMAE = 0.72). Despite this, modelled $PM_{2.5}$ concentrations captured the variability and magnitude of peaks seen in the observations across eastern-Australia and for specific cities.

We find that between September and February large proportions of the population were exposed to dangerous (‘Poor’,’V.Poor’ and ‘Hazardous’) air quality levels. In total, the fires led to an additional ~1.9 million people being exposed to ‘Poor’ or worse AQI values on average (~1.1 million exposed to ‘Poor’, 437,000 to ‘V.Poor’ and 339,000 to ‘Hazardous’ AQI values) across eastern Australia between September and the end of January, compared to if there were no fires. The impact of the bushfires on AQ was concentrated in the cities of Sydney, Newcastle-Maitland and Canberra-Queanbeyan during November, December and, also in Melbourne, in January. While, generally Brisbane and Adelaide were less severely affected by the fires.

We estimate the health impacts of exposure to $PM_{2.5}$ from fires across eastern-Australia, at regional and city level using a short-term exposure response function (World Health Organization, 2013). Our estimate indicates that between October and February 171 (95% CI: 64 – 277) deaths were brought forward due to the fires, 624 (95% CI: 230 – 1008) due to all $PM_{2.5}$ and 456 (95% CI: 169 – 738) if there were no fires. The health impacts were largest in New South Wales, Queensland and Victoria with 109 (95% CI: 41 – 176), 15 (95% CI: 5 – 24) and 35 (95% CI: 13 – 56) deaths brought forward due to fires in these regions (287 (95% CI:107 – 463), 112 (95% CI: 41 – 181) and 155 (95% CI: 57 – 250) all $PM_{2.5}$), respectively. Our results lie within the range of estimated bushfire $PM_{2.5}$ health impacts from both Borchers Arriagada *et al.* (2020) and Ryan *et al.* (2021) for New South Wales but below the lower limit for other regions, such as Victoria. This is most likely due to differences in how bushfire $PM_{2.5}$ was estimated in each study and also differences in the estimated population-weighted bushfire $PM_{2.5}$ concentrations. This study builds upon previous work by using an atmospheric chemistry transport model to isolate the impacts of the fires on air quality and also to investigate the impacts regionally, away from observational sites. At a city-level, the health impacts of $PM_{2.5}$ exposure due to fires were concentrated in the cities with large populations and high $PM_{2.5}$ concentrations due to fires. The highest number of deaths brought forward due to short-term bushfire $PM_{2.5}$ exposure were in Sydney (65 (95% CI: 24 – 105)), Melbourne (23 (95% CI: 9 – 38)) and Canberra-Queanbeyan (9 (95% CI: 4 – 14).

This work confirms that there was a substantial AQ and health impact across eastern-Australia from the 2019/2020 bushfires. Our study only considered mortality, therefore the full health impact of exposure to $PM_{2.5}$ is likely to be higher and requires further studies addressing the impacts on hospital admissions, ambulance call outs and primary health care visits. Alongside this, the impact of other pollutants on health could also be quantified. In the future, further work is required to characterise the health impacts of exposure to pollutants from wildfires. This would allow for more comprehensive estimates of the health impacts associated with population exposure. Finally, with more dry years like 2019/2020 projected to occur in the future due to climate change the impact of wildfires such as 2019/2020 are likely to be seen again. Therefore, fire risk management policies should be developed further to consider the impact of climate change on wildfire frequency and intensity across the country.

Acknowledgments, Samples, and Data

This work was supported by the UK Natural Environment Research Council (NERC) by providing funding for the National Centre for Earth Observation (NCEO), Grant No. NE/R016518/1.

Observations of $PM_{2.5}$ were accessed from the https://www.dpie.nsw.gov.au/air-quality/air-quality-concentration-data-updated-hourly, https://discover.data.vic.gov.au/dataset/epa-air-watch-all-sites-air-quality-hourly-averages-yearly/historical, https://www.data.qld.gov.au/dataset/air-quality-monitoring-2019/resource/c9ecf021-faa4-4d5a-93c7-7460c083d682 and https://www.data.act.gov.au/Environment/Air-Quality-Monitoring-Data/94a5-zqnn . Gridded population data for 2018 was accessed from the Australia Bureau of Statistics https://www.abs.gov.au/AUSSTATS/abs@.nsf/DetailsPage/3218.02017-18?OpenDocument. All-cause mortality data for 2018 was taken from the Australia Bureau of Statistics http://stat.data.abs.gov.au/Index.aspx?DataSetCode=DEATHS_AGESPECIFIC_OCCURENCEYEAR. We acknowledge use of the Weather Research and Forecasting model coupled with Chemistry preprocessor tool mozbc, fire_emiss, bio_emiss and anthro_emis provided by the Atmospheric Chemistry Observations and Modeling Lab (ACOM) of NCAR. We acknowledge use of the postprocessing script “wrfout_to_cf.ncl” created by Mark Seefeldt at the University of Colorado at Boulder (http://foehn.colorado.edu/wrfout_to_cf/). The Supplementary Material contains all results and further information on our analysis. As far as we are aware there are no competing financial interests.

Code to setup and run WRFChem (using WRFotron version 2.0) is available through Conibear and Knote (2020). WRF-Chem simulation data will be made available from the Research Data Leeds Repository (http://archive.researchdata.leeds.ac.uk/) by acceptance.

Author Contributions

- Ailish Graham – conceptualization, methodology, software, formal analysis, data curation and writing (original and review), visualisation and investigation with help and guidance from Stephen Arnold, Richard Pope, Kirsty Pringle and James McQuaid.
- Supervision - Stephen Arnold, Richard Pope, Kirsty Pringle, James McQuaid.
- Funding acquisition - James McQuaid.
- Fire emissions data - Edward Butt.
- Post-processing scripts - Luke Conibear.
- Fire emissions scaling advice, simulation advice – Laura Kiely, Carly Reddington, Edward Butt, Luke Conibear, Matthew Woodhouse and Dominick Spracklen.
- Health Impact Assessment advice – Nicolás Borchers Arriagada
- WRF-Chem set-up and automation scripts – Christoph Knote
- HPC model set-up, model de-bugging and computing support – Helen Burns and Richard Rigby.

References

Akagi, S.K., Yokelson, R.J., Wiedinmyer, C., Alvarado, M.J., Reid, J.S., Karl, T., Crounse, J.D., Wennberg, P.O., 2011. Emission factors for open and domestic biomass burning for use in atmospheric models. Atmos. Chem. Phys. 11, 4039–4072. https://doi.org/10.5194/acp-11-4039-2011

Andreae, M.O., Melret, P., Merlet, P., Metlet, P., 2001. Emission of trace gases and aerosols from biomass burning. Global Biogeochem. Cycles 15, 955–966. https://doi.org/10.1029/2000GB001382

Archer-Nicholls, S., Lowe, D., Darbyshire, E., Morgan, W.T., Bela, M.M., Pereira, G., Trembath, J., Kaiser, J.W., Longo, K.M., Freitas, S.R., Coe, H., McFiggans, G., 2015. Characterising Brazilian biomass burning emissions using WRF-Chem with MOSAIC sectional aerosol. Geosci. Model Dev. 8, 549–577. https://doi.org/10.5194/gmd-8-549-2015

Australia State of the Environment, 2016. Vegetation.

Australian Bureau of Meteorology, 2020. Australian Climate Influences: IOD [WWW Document]. URL http://www.bom.gov.au/climate/about/?bookmark=iod

Australian Bureau of Meteorology, 2019a. Tracking Australia's climate through 2019 [WWW Document]. URL http://www.bom.gov.au/climate/updates/articles/a036.shtml

Australian Bureau of Meteorology, 2019b. Southern Annular Mode [WWW Document]. URL http://www.bom.gov.au/climate/about/?bookmark=sam

Australian Bureau of Statistics, 2020. Deaths, Year of occurrence, Age at death, Age-specific death rates, Sex, States, Territories and Australia [WWW Document]. URL http://stat.data.abs.gov.au/Index.aspx?DataSetCode=DEATHS_AGESPECIFIC_OCCURENCEYEAR (accessed 1.7.21).

Australian Bureau of Statistics, 2019. Regional Population Growth, Australia, 2017-18 [WWW Document]. URL https://www.abs.gov.au/AUSSTATS/abs@.nsf/DetailsPage/3218.02017-18?OpenDocument (accessed 1.7.21).

Black, C., Tesfaigzi, Y., Bassein, J.A., Miller, L.A., 2017. Wildfire smoke exposure and human health: Significant gaps in research for a growing public health issue. Environ. Toxicol. Pharmacol. 55, 186–195. https://doi.org/10.1016/j.etap.2017.08.022

Boer, M., Resco de Dios, V., Bradstock, R., 2020. Unprecedented burn area of Australian mega forest fires. Nat. Clim. Chang. 10, 170. https://doi.org/10.1038/s41558-020-0710-7

Borchers Arriagada, N., Palmer, A.J., Bowman, D.M.J.S., Morgan, G.G., Jalaludin, B.B., Johnston, F.H., 2020. Unprecedented smoke-related health burden associated with the 2019–20 bushfires in eastern Australia. Med. J. Aust. 2019–2020. https://doi.org/10.5694/mja2.50545

Brew, N., Richards, L., Smith, L., 2020. 2019–20 Australian bushfires—frequently asked questions: a quick guide.

Conibear, L., Butt, E., Knote, C., Arnold, S., Spracklen, D., 2018a. Residential energy use emissions dominate health impacts from exposure to ambient particulate matter in India. Nat. Commun. 9, 1–9. https://doi.org/10.1038/s41467-018-02986-7

Conibear, L., Butt, E., Knote, C., Arnold, S., Spracklen, D., 2018b. Stringent Emission Control Policies Can Provide Large Improvements in Air Quality and Public Health in

India. GeoHealth 2, 196–211. https://doi.org/10.1029/2018gh000139

Conibear, L., Butt, E., Knote, C., Spracklen, D., Arnold, S., 2018c. Current and Future Disease Burden From Ambient Ozone Exposure in India. GeoHealth 2, 334–355. https://doi.org/10.1029/2018gh000168

Conibear, L., Knote, C., 2020. WRFotron [WWW Document]. URL https://agupubs.onlinelibrary.wiley.com/doi/full/10.1029/2021GH000391#gh2231-bib-0010

Crippa, P., Castruccio, S., Archer-Nicholls, S., Lebron, G., Kuwata, M., Thota, A., Sumin, S., Butt, E., Wiedinmyer, C., Spracklen, D., 2016. Population exposure to hazardous air quality due to the 2015 fires in Equatorial Asia. Sci. Rep. 6, 1–9. https://doi.org/10.1038/srep37074

Delfino, R.J., Brummel, S., Wu, J., Stern, H., Ostro, B., Lipsett, M., Winer, A., Street, D.H., Zhang, L., Tjoa, T., Gillen, D.L., Ostro, B., Zhang, L., Street, D.H., Lipsett, M., Brummel, S., Delfino, R.J., Gillen, D.L., Stern, H., 2009. The relationship of respiratory and cardiovascular hospital admissions to the southern California wildfires of 2003. Occup. Environ. Med. 66, 189–197. https://doi.org/10.1136/oem.2008.041376

Emmons, L.K., Walters, S., Hess, P.G., Lamarque, J.-F., Pfister, G.G., Fillmore, D., Granier, C., Guenther, A., Kinnison, D., Laepple, T., Orlando, J., Tie, X., Tyndall, G., Wiedinmyer, C., Baughcum, S.L., Kloster, S., 2009. Description and evaluation of the Model for Ozone and Related chemical Tracers, version 4 (MOZART-4). Geosci. Model Dev. Discuss. 2, 1157–1213. https://doi.org/10.5194/gmdd-2-1157-2009

Faustini, A., Alessandrini, E.R., Pey, J., Perez, N., Samoli, E., Querol, X., Cadum, E., Perrino, C., Ostro, B., Ranzi, A., Sunyer, J., Stafoggia, M., Forastiere, F., Angelini, P., Berti, G., Bisanti, L., Catrambone, M., Chiusolo, M., Davoli, M., De'donato, F., Demaria, M., Gandini, M., Grosa, M., Ferrari, S., Pandolfi, P., Pelosini, R., Pietrodangelo, A., Pizzi, L., Poluzzi, V., Priod, G., Randi, G., Rowinski, M., Scarinzi, C., Stivanello, E., Zauli-Sajani, S., Dimakopoulou, K., Elefteriadis, K., Katsouyanni, K., Kelessis, A., Maggos, T., Michalopoulos, N., Pateraki, S., Petrakakis, M., Rodopoulou, S., Sypsa, V., Agis, D., Artiñano, B., Barrera-Gómez, J., Basagaña, X., De La Rosa, J., Diaz, J., Fernandez, R., Jacquemin, B., Karanasiou, A., Linares, C., Sanchez, A.M., Tobias, A., Bidondo, M., Declercq, C., Le Tertre, A., Lozano, P., Medina, S., Pascal, L., Pascal, M., 2015. Short-term effects of particulate matter on mortality during forest fires in Southern Europe: Results of the MED-PARTICLES project. Occup. Environ. Med. 72, 323–329. https://doi.org/10.1136/oemed-2014-102459

Freitas, S.R., Longo, K.M., Chatfield, R., Latham, D., Silva Dias, M.A.F., Andreae, M.O., Prins, E., Santos, J.C., Gielow, R., Carvalho, J.A., 2007. Including the sub-grid scale plume rise of vegetation fires in low resolution atmospheric transport models. Atmos. Chem. Phys. 7, 3385–3398. https://doi.org/10.5194/acp-7-3385-2007

Hoelzemann, J.J., Schultz, M.G., Brasseur, G.P., Granier, C., Simon, M., 2004. Global Wildland Fire Emission Model (GWEM): Evaluating the use of global area burnt satellite data. J. Geophys. Res 109, 14–18. https://doi.org/10.1029/2003JD003666

Hoffmann, L., Günther, G., Li, D., Stein, O., Wu, X., Griessbach, S., Heng, Y., Konopka, P., Müller, R., Vogel, B., Wright, J.S., 2018. From ERA-Interim to ERA5: considerable impact of ECMWF's next-generation reanalysis on Lagrangian transport simulations. Atmos. Chem. Phys. Discuss. 1–38. https://doi.org/10.5194/acp-2018-1199

Holgate, S., 1998. Quantification ofthe Effects ofAir Pollution on Health in the United Kingdom. The Stationary Office, London.

Janssens-Maenhout, G., Crippa, M., Guizzardi, D., Dentener, F., Muntean, M., Pouliot, G., Keating, T., Zhang, Q., Kurokawa, J., Wankmüller, R., Denier Van Der Gon, H., Kuenen, J.J.P., Klimont, Z., Frost, G., Darras, S., Koffi, B., Li, M., 2015. HTAP-v2.2: A mosaic of regional and global emission grid maps for 2008 and 2010 to study hemispheric transport of air pollution. Atmos. Chem. Phys. 15, 11411–11432. https://doi.org/10.5194/acp-15-11411-2015

Jenner, L., 2020. From Smoke Going Round the World to Aerosol Levels, NASA Observes Australia's Bushfires [WWW Document]. NASA.

Johnston, F., Hanigan, I., Henderson, S., Morgan, G., Bowman, D., 2011. Extreme air pollution events from bushfires and dust storms and their association with mortality in Sydney, Australia 1994-2007. Environ. Res. 111, 811–816. https://doi.org/10.1016/j.envres.2011.05.007

Johnston, F.H., Henderson, S.B., Chen, Y., Marlier, M., DeFries, R.S., Kinney, P., Bowman, D.M.J.S., Randerson, J.T., Marlier, M., DeFries, R.S., Kinney, P., Bowman, D.M.J.S., Brauer, M., 2012. Estimated global mortality attributable to smoke from landscape fires. Environ. Health Perspect. 120, 695–701. https://doi.org/10.1289/ehp.1104422

Kiely, L., Spracklen, D. V., Wiedinmyer, C., Conibear, L., Reddington, C.L., Archer-Nicholls, S., Lowe, D., Arnold, S.R., Knote, C., Firoz Khan, M., Talib Latif, M., Kuwata, M., Hapsari Budisulistiorini, S., Syaufina, L., 2019. New estimate of particulate emissions from Indonesian peat fires in 2015. Atmos. Chem. Phys. 19, 11105–11121. https://doi.org/10.5194/acp-19-11105-2019

Kiely, L., Spracklen, D. V, Wiedinmyer, C., Conibear, L.A., Reddington, C.L., Arnold, S.R., Knote, C., Khan, M.F., Latif, M.T., Syaufina, L., Adrianto, H.A., 2020. Air quality and health impacts of vegetation and peat fires in Equatorial Asia during 2004 – 2015. Environ. Res. Lett. https://doi.org/10.1088/1748-9326/ab9a6c

Lee, H., 2019. Bushfires Release Over Half Australia's Annual Carbon Emissions. Bloom. Green.

Lelieveld, J., Evans, J.S., Fnais, M., Giannadaki, D., Pozzer, A., 2015. The contribution of outdoor air pollution sources to premature mortality on a global scale. Nature 525, 367–371. https://doi.org/10.1038/nature15371

Liu, J.C., Pereira, G., Uhl, S.A., Bravo, M.A., Bell, M.L., 2015. A systematic review of the physical health impacts from non-occupational exposure to wildfire smoke. Environ. Res. 136, 120–132. https://doi.org/10.1016/j.envres.2014.10.015

Lucas, C., Hennessy, K., Mills, G., Bathols, J., 2007. Bushfire Weather in Southeast Australia : Recent Trends and Projected Climate Change Impacts. Consult. Rep. Prep. Clim. Inst. Aust. 84.

Macintyre, H.L., Heaviside, C., Neal, L.S., Agnew, P., Thornes, J., Vardoulakis, S., 2016. Mortality and emergency hospitalizations associated with atmospheric particulate matter episodes across the UK in spring 2014. Environ. Int. 97, 108–116. https://doi.org/10.1016/j.envint.2016.07.018

Marsh, D.R., Mills, M.J., Kinnison, D.E., Lamarque, J.F., Calvo, N., Polvani, L.M., 2013. Climate change from 1850 to 2005 simulated in CESM1(WACCM). J. Clim. 26, 7372–7391. https://doi.org/10.1175/JCLI-D-12-00558.1

Mcmeeking, G.R., 2008. The Optical, Chemical, and Physical Properties of Aerosols and Gases Emitted by the Laboratory Combustion of Wildland Fires 321.

Naeher, L.P., Brauer, M., Lipsett, M., Zelikoff, J.T., Simpson, C.D., Koenig, J.Q., Smith, K.R., 2007. Woodsmoke health effects: A review. Inhal. Toxicol. 19, 67–106. https://doi.org/10.1080/08958370600985875

Olivier, J., Peters, J., Granier, C., Pétron, G., Müller, J., Wallens, S., ;, 2003. Present and future surface emissions of atmospheric compounds.

Pope, R.J., Kerridge, B.J., Siddans, R., Latter, B.G., Chipperfield, M.P., Arnold, S.R., Ventress, L.J., Pimlott, M.A., Graham, A.M., Knappett, D.S., Rigby, R., 2021. Large enhancements in southern hemisphere satellite-observed trace gases due to the 2019/2020 Australian wildfires. J. Geophys. Res. Atmos. 16. https://doi.org/10.1002/essoar.10507019.1

Reddington, C., Conibear, L., Knote, C., Silver, B., Li, Y., Chan, C., Arnold, S., Spracklen, D., 2019. Exploring the impacts of anthropogenic emission sectors on PM2.5 and human health in South and East Asia. Atmos. Chem. Phys. 19, 11887–11910. https://doi.org/10.5194/acp-19-11887-2019

Reid, C.E., Brauer, M., Johnston, F.H., Jerrett, M., Balmes, J.R., Elliott, C.T., E., R.C., Michael, B., H., J.F., Michael, J., R., B.J., T., E.C., 2016. Critical review of health impacts of wildfire smoke exposure. Environ. Health Perspect. 124, 1334–1343. https://doi.org/10.1289/ehp.1409277

Ryan, R.G., Silver, J.D., Schofield, R., 2021. Air quality and health impact of 2019-20 Black Summer Megafires and COVID-19 lockdown in Melbourne and Sydney, Australia. Environ. Pollut. 116498. https://doi.org/10.1016/j.envpol.2021.116498

Schmidt, A., Ostro, B., Carslaw, K.S., Wilson, M., Thordarson, T., Mann, G.W., Simmons, A.J., 2011. Excess mortality in Europe following a future Laki-style Icelandic eruption.

Proc. Natl. Acad. Sci. 108, 15710–15715. https://doi.org/10.1073/pnas.1108569108

Silver, B., Conibear, L., Reddington, C., Knote, C., Arnold, S., Spracklen, D., 2020. Pollutant emission reductions deliver decreased PM_{2.5}-caused mortality across China during 2015–2017. Atmos. Chem. Phys. 2017, 1–18. https://doi.org/10.5194/acp-2019-1141

Sutton, M.A., van Grinsven, H., Billen, G., Bleeker, A., Bouwman, A.F., Bull, K., Erisman, J.W., Grennfelt, P., Grizzetti, B., Howard, C.M., Oenema, O., Spranger, T., Winiwarter, W., 2011. Summary for policy makers. Eur. Nitrogen Assess. xxiv–xxxiv. https://doi.org/10.1017/cbo9780511976988.002

UCAR, 2020a. WRF-Chem MOZART-4 DOWNLOAD [WWW Document]. URL https://www.acom.ucar.edu/wrf-chem/mozart.shtml (accessed 9.16.20).

UCAR, 2020b. WACCM Download [WWW Document]. URL https://www.acom.ucar.edu/waccm/download.shtml (accessed 9.16.20).

van Oldenborgh, G.J., Krikken, F., Lewis, S., Leach, N., Lehner, F., Saunders, K., van Weele, M., Haustein, K., Li, S., Wallom, D., Sparrow, S., Arrighi, J., Singh, R., van Aalst, M., Philip, S., Vautard, R., Otto, F., 2020. Attribution of the Australian bushfire risk to anthropogenic climate change. Nat. Hazards Earth Syst. Sci. 1–46. https://doi.org/10.5194/nhess-2020-69

Verzoni, A., 2021. Wildlife Toll [WWW Document]. Natl. Fire Prot. Assoc.

Wiedinmyer, C., Akagi, S.K., Yokelson, R.J., Emmons, L.K., Al-Saadi, J.A., Orlando, J.J., Soja, A.J., 2011. The Fire INventory from NCAR (FINN): a high resolution global model to estimate the emissions from open burning. Geosci. Model Dev. 4, 625–641.

https://doi.org/10.5194/gmd-4-625-2011

Wintle, B.A., Legge, S., Woinarski, J.C.Z., 2020. After the Megafires: What Next for Australian Wildlife? Trends Ecol. Evol. xx, 1–5. https://doi.org/10.1016/j.tree.2020.06.009

World Health Organization, 2013. Health risks of air pollution in Europe – HRAPIE project. World Heath Organ. 60.

Zanobetti, A., Schwartz, J., 2009. The effect of fine and coarse particulate air pollution on mortality: A national analysis. Environ. Health Perspect. 117, 898–903. https://doi.org/10.1289/ehp.0800108

Zaveri, R.A., Easter, R.C., Fast, J.D., Peters, L.K., 2008. Model for Simulating Aerosol Interactions and Chemistry (MOSAIC). J. Geophys. Res. Atmos. 113, 1–29. https://doi.org/10.1029/2007JD008782